

University of Groningen

Stabilizing Single Atom Contacts by Molecular Bridge Formation

Huisman, Everardus H.; Trouwborst, Marius L.; Bakker, Frank L.; de Boer, Bert; van Wees, Bart; van der Molen, Sense J.

Published in:
 Nano Letters

DOI:
[10.1021/nl801983z](https://doi.org/10.1021/nl801983z)

IMPORTANT NOTE: You are advised to consult the publisher's version (publisher's PDF) if you wish to cite from it. Please check the document version below.

Document Version
 Publisher's PDF, also known as Version of record

Publication date:
 2008

[Link to publication in University of Groningen/UMCG research database](#)

Citation for published version (APA):

Huisman, E. H., Trouwborst, M. L., Bakker, F. L., de Boer, B., van Wees, B. J., & van der Molen, S. J. (2008). Stabilizing Single Atom Contacts by Molecular Bridge Formation. *Nano Letters*, 8(10), 3381-3385.
 DOI: 10.1021/nl801983z

Copyright

Other than for strictly personal use, it is not permitted to download or to forward/distribute the text or part of it without the consent of the author(s) and/or copyright holder(s), unless the work is under an open content license (like Creative Commons).

Take-down policy

If you believe that this document breaches copyright please contact us providing details, and we will remove access to the work immediately and investigate your claim.

Downloaded from the University of Groningen/UMCG research database (Pure): <http://www.rug.nl/research/portal>. For technical reasons the number of authors shown on this cover page is limited to 10 maximum.

SUPPORTING INFORMATION

Stabilizing single atom contacts by molecular bridge formation

August 18, 2008

Everardus H. Huisman, Marius L. Trouwborst, Frank L. Bakker, Bert de Boer, Bart J. van Wees and Sense J. van der Molen

*Zernike Institute for Advanced Materials, University of Groningen, Nijenborgh 4, 9747 AG Groningen, The Netherlands, and Kamerlingh Onnes Laboratory, Leiden University, Niels Bohrweg 2, 2333 CA Leiden, The Netherlands*¹

General considerations Toluene, was passed over columns of Al₂O₃ (Fluka), BASF R3-11-supported Cu oxygen scavenger, and molecular sieves (Aldrich, 4 Å). In order to exclude water and oxygen, solutions are kept under nitrogen or argon. All areas that were exposed to solvents (tubing, syringes, bottles, septa) are made of Teflon or glass and have been cleaned in Merck Extran Soap, demi water, acetone and 2-propanol using ultrasonic baths, blown dry and stored in an oven at 150 °C. For each experiment, a small amount of dithiols (as received) was weighed in a bottle under ambient conditions. Then the bottle was sealed with a septa, purged with nitrogen and a 10 mM thiol solution in toluene was made under nitrogen. Solutions can be applied to the setup using syringes. Syringes were rinsed with argon and filled using septa-capped bottles under argon. After adding alkanethiols, a sample cannot be used for other thiol experiments since due to incomplete exchange of thiols on the gold surface.

MCBJ set-up with a liquid cell In order to have a liquid environment we mounted a liquid cell on top of the MCBJ. The reservoir has inlets and

¹†University of Groningen ‡University of Leiden and University of Groningen Corresponding author email address: e.h.huisman@rug.nl

outlets, such that liquids and gases can be applied. Figure 1 gives a detailed description of the set-up.

Determination of ζ ζ was determined by recording the conductance when closing the junctions in argon while the liquid cell was mounted. Figure 2 shows 3 closing traces in the out-of-contact regime of 3 different samples on a semilog plot. Since $G \propto \exp(-2\kappa \cdot r \cdot Z)$, the slope of these lines, $dy/dx = d^{10} \log(G_0)/dZ = d^{10} \log(\exp(-2 \cdot \kappa \cdot r \cdot Z))/dZ = -2 \cdot \kappa \cdot r \cdot^{10} \log(e)$. Therefore, $\kappa = (dy/dx)/(-2 \cdot^{10} \log(e) \cdot r)$. Assuming a workfunction of gold, $\phi = 5.3eV$, one can determine a reference, $\kappa_{ref} = \frac{\sqrt{2m\phi}}{\hbar} = 11.8nm^{-1}$. Taking the average slope of the three lines for each sample, one finds, $dy/dx =^{10} \log(G_0)/dZ = 0.63 \pm 0.1$, 0.63 ± 0.1 and $1.1 \pm 0.1dec/\mu m$, yielding an average slope of $0.79 \pm 0.1 dec/\mu m$. This gives $\kappa = 53 \pm 13 nm^{-1}$ and $\zeta = \kappa/\kappa_{ref} = 4.5 \pm 0.6$.

Determination of the electrode drift We have measured the drift of the electrodes in toluene at room temperature, see Figure 3. When opened, the resistance at a constant bias of 100mV decreases from 1 M Ω to 300 k Ω in 1 hour. Assuming direct tunneling and using a workfunction of gold of 5.3 eV (solvent molecules cannot really be in between the tips of the electrodes at these distances), one can relate this resistance change to a distance change of about 50 pm. In 1 hour this corresponds to a drift of less than 1pm/min. Also, sudden jumps randomly in time are visible in the measurements. These resistance jumps correspond to a sudden distance change of the electrodes of a fraction of the size of an atom. Since alike jumps were also observed without solvent in argon or air, we attribute these jumps to surface adatom diffusion.

Histogram evolution as a function of the number of traces To investigate the dependance of the appearance of the histogram on the number of traces, we have constructed logarithmic histograms with different amounts of traces. Figure 4 shows a histogram of sample BDT1 (see main text for details) containing 100, 200 and 300 traces respectively. No clear changes in the distribution of counts occur as a function of number of traces. Furthermore, the number of counts increases roughly linearly with increasing trace number.

Histograms of the contact regime To investigate the increase of counts around 1 G_0 in more detail, we constructed linear histograms for the contact regime, see Figure 5. Both the histogram for toluene (black), ODT (red) and

BDT (green) are shown. Clearly, the maximum of the $1G_0$ peak increases when adding alkanedithiol molecules to the solution. For all experiments performed, the peak decays faster on the high conductance side than on the low conductance side. This indicates well defined contacts in agreement with previous reports.

Histograms of the additional measurements Figure 6 shows the linear histogram and representative traces for the additional measurements of sample TOL3, ODT2 and BDT2.

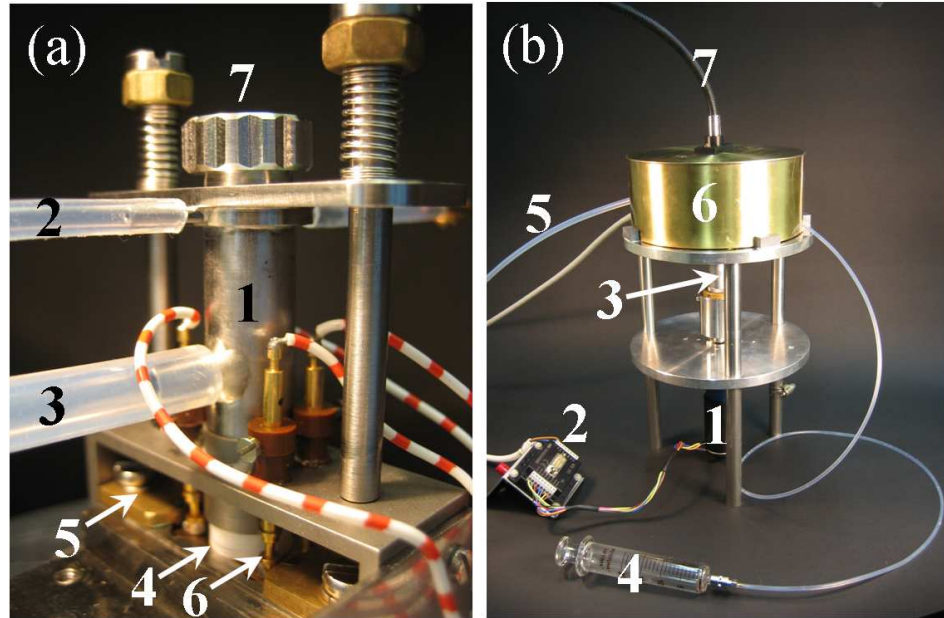


Figure 1: Photographs of the MCBJ setup containing a liquid cell. **(a)** A photograph of the set-up near the three point bending mechanism. A 2 ml stainless steel Teflon coated reservoir (1) containing an inlet (2) and an outlet (3) is mounted on top of the MCBJ using a Gore foam sealing ring (4). The pushing rod is coming from below and the substrate is clamped by the counter supports (5). Electrical contact between sample and leads is realized by using spring loaded contacts with an indium tip (6). The setup is equipped with a quartz window for optical access for future purposes. **(b)** A photograph of the whole set up. The pushing rod is controlled by a Faulhaber brushless servo motor (1) equipped with a gearbox. The motor is controlled by a computer using a motor controller (2) connected to the serial port of the computer. The motor is attached to a Mitotoyu micrometer screw (3) (1 rev = 50 μm). Solutions can be supplied via a syringe (4) connected to the inlet. The outlet (5) can be connected either to a vacuum system or to a bubbler. The setup is shielded from environmental noise by a Faraday cage (6). Light can be applied to the set-up using a glass fiber (7) for future purposes.

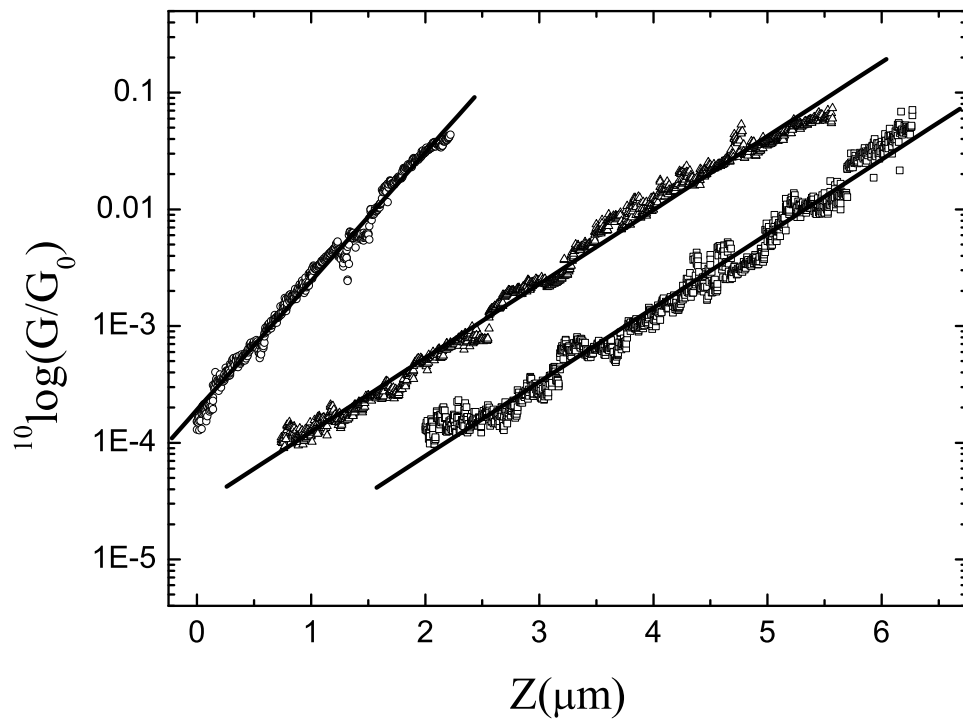


Figure 2: 3 closing traces for 3 different samples on a semilog plot. The traces are recorded in argon while the liquid cell is mounted. ζ can be determined from the slope of the traces. The traces have an offset in the x-axis for better visibility.

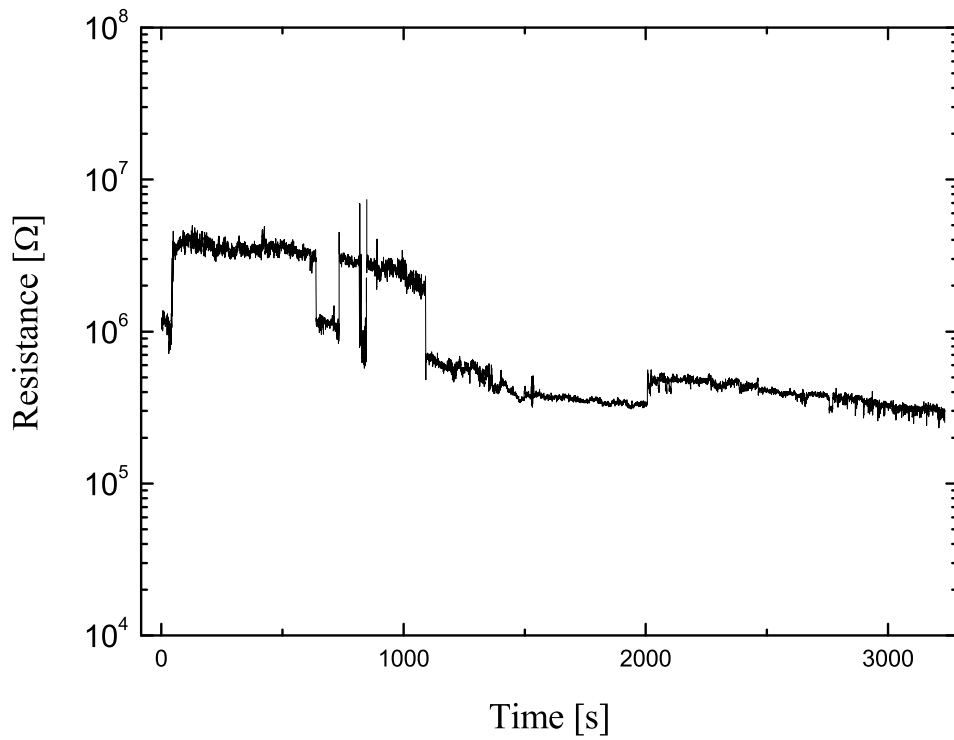


Figure 3: The resistance of a break junction at fixed motor position in the out of contact regime as a function of time. The sample is emerged in toluene at room temperature. A linear drift and sudden jumps in the resistance are observable. The linear drift corresponds to an electrode displacement of less than 1 pm/min. We attribute the sudden jumps to surface adatom diffusion.

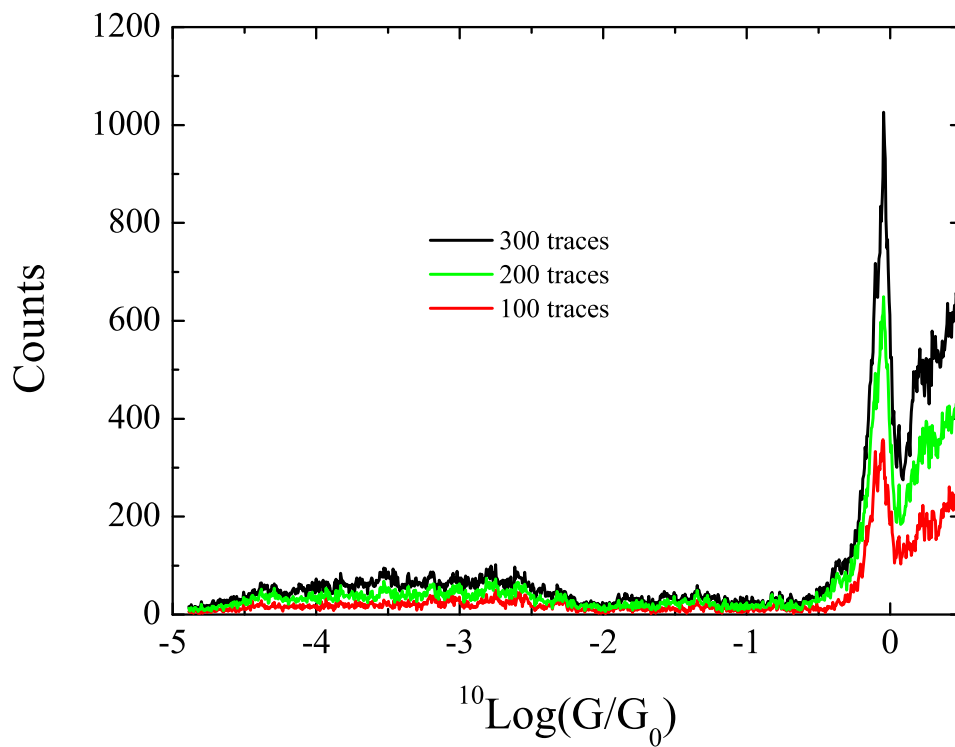


Figure 4: 3 opening conductance histograms of BDT1 with 100, 200 and 300 traces, respectively. No changes in the distribution of counts occur as a function of trace number occur. The number of counts increases linearly with increasing trace number.

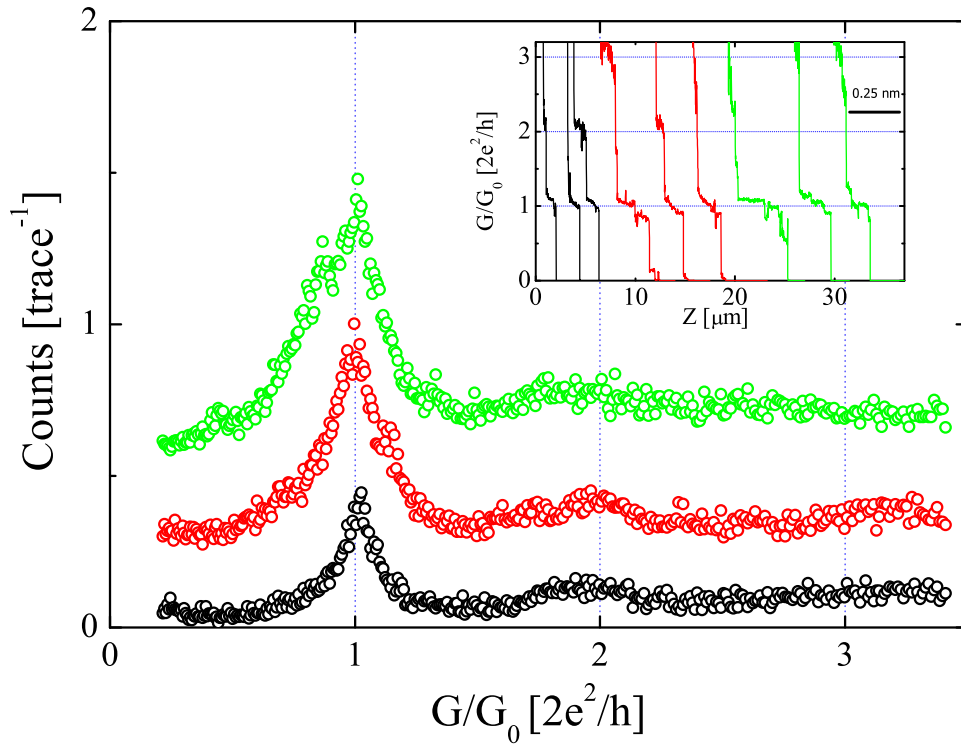


Figure 5: Linear conductance histogram of 250 opening traces in toluene of sample TOL1 (black), 300 opening traces in 10 mM ODT of sample ODT1 (red) and 300 opening traces in 10 mM BDT of sample BDT1 (green). The histograms were normalized by dividing the counts by the number of traces for each experiment. The traces are displaced in y for clarity. The inset displays 3 sample traces for each solution. The scale bar shows the actual electrode displacement d .

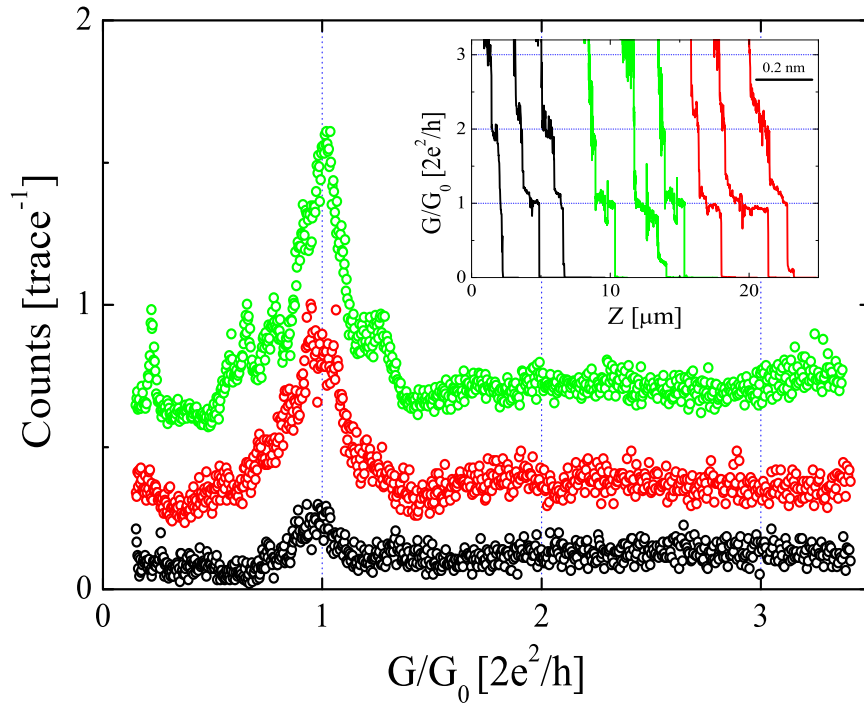


Figure 6: Linear conductance histogram. of 150 opening traces in toluene of sample TOL3 (black), 150 opening traces in 10 mM ODT of sample ODT2 (red) and 50 opening traces in 10 mM BDT of sample BDT2 (green). The histograms were normalized by dividing the counts by the number of traces for each experiment. The traces are displaced in y for clarity. The inset displays 3 sample traces for each solution. The scale bar shows the actual electrode displacement d .